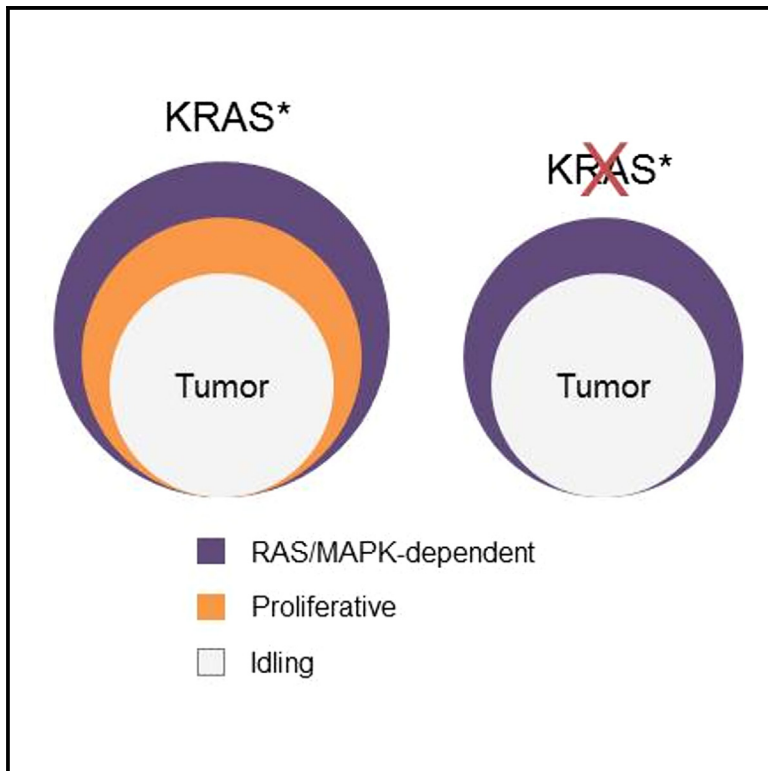# Intratumor heterogeneity in KRAS signaling shapes treatment resistance

Graphical abstract

Authors

Oleksi Petrenko, Varvara Kirillov,
Stephen D'Amico, Nancy C. Reich

Correspondence

alexei.petrenko@stonybrook.edu (O.P.),
nancy.reich@stonybrook.edu (N.C.R.)

In brief

Cell biology; Cancer; Omics

Highlights

- PDAC tumors display mixtures of cells with various degrees of KRAS dependency

- Oncogenic KRAS dependency is an essential feature of proliferating cells

- Intrinsic KRAS independence confers a drug-resistant idling phenotype

- Combination immunotherapy leads to tumor regression in preclinical models

CellPress

Intratumor heterogeneity in KRAS signaling shapes treatment resistance

Oleksi Petrenko,[1,*] Varvara Kirillov,[1] Stephen D'Amico,[1] and Nancy C. Reich[1,2,*]

[1]Department of Microbiology and Immunology, Stony Brook University, Stony Brook, NY, USA
[2]Lead contact
*Correspondence: alexei.petrenko@stonybrook.edu (O.P.), nancy.reich@stonybrook.edu (N.C.R.)
https://doi.org/10.1016/j.isci.2024.111662

SUMMARY

KRAS mutations are linked to some of the deadliest forms of cancer. Pharmacological studies suggest that co-targeting KRAS with feedback/bypass pathways could lead to enhanced anti-tumor activity. The underlying premise is that cancers display a deep-rooted hypersensitivity to KRAS inactivation. Here, we investigate the role of intratumor heterogeneity in pancreatic ductal adenocarcinoma, focusing on oncogenic KRAS addiction and treatment resistance. Integrated analysis of single-cell and bulk RNA sequencing data reveals that most tumors display a mixture of cells with vastly different degrees of KRAS dependency. We identify distinct cell populations that vary in their gene expression patterns pertaining to the predicted level of KRAS signaling activity, cell growth, and differentiation commitment within each tumor. Selective targeting of mutant KRAS suppresses the growth of tumor cells with high RAS/mitogen-activated protein kinase (MAPK) activity while sparing pre-existing subsets with low RAS signaling activity, necessitating alternative treatments. Combination immunotherapy leads to durable tumor regression in preclinical models.

INTRODUCTION

KRAS is the most frequently mutated oncogene in cancer. KRAS activates multiple effector pathways, including the mitogen-activated protein kinase (MAPK), phosphatidylinositol 3-kinase (PI3K), RHO, and RAL pathways, but their limited understanding hampers targeted therapies. Clinical efforts have focused on blocking KRAS itself or its effector pathways that regulate cell growth. The central theme has been that most cancers acquire resistance to KRAS inhibition and ultimately relapse. There are several issues to consider. First, about half of cancers treated with KRAS[G12C] inhibitor monotherapy acquired mutations in tumor suppressor genes (KEAP1, SMARCA4, and CDKN2A) or PI3K and RAS family genes.[1–4] Therefore, the role and contribution of the mutation rate in cancer have been underestimated.[5] Second, a broad array of stress response and bypass mechanisms has been proposed to replace KRAS both before and after treatment.[6–9] Adaptive feedback reactivation of RAS/MAPK signaling has been touted as a key mediator of acquired resistance.[10–12] Some pathways may, indeed, exert anti-apoptotic effects following KRAS inhibition. However, they are not sufficient to elicit tumorigenic changes. There is ample evidence that KRAS plays key roles in both cancer growth and therapy and that resistance is more likely to arise within than alongside KRAS.[2,13,14] Regardless of this, many post-treatment tumors display no newly acquired mutations, suggesting that the resistance to KRAS inhibitors can be more multifaceted.

Against this background, several prior studies have shown that cancer cells bearing KRAS mutations can be classified into two groups: KRAS dependent (termed KRAS-type) and

KRAS independent (RSK-type).[15,16] KRAS-dependent cells are addicted specifically to KRAS itself and RAF/MAPK signaling, while cells that are nominally KRAS independent curtail MAPK activation but exhibit enhanced dependency on the RSK/MTOR pathway.[16,17] Furthermore, as we have previously found, one-third of pancreatic tumors could not be stratified into these two major subtypes of cancer, dependent on KRAS or RSK.[18] This raised the question about the heterogeneity of KRAS signaling and whether the intrinsic mechanisms of resistance could account for the apparent lack of response in clinical trials.

In this study, we investigate the intratumor heterogeneity of KRAS signaling activity, since it underlies each of the aspects listed earlier (i.e., oncogenic dependency and the clinical outcome). Here, we propose that keeping the balance between self-renewal (proliferation) and cell-cycle arrest (differentiation) is a defining property of KRAS-driven tumors. Cross-species analysis of single-cell and bulk RNA sequencing data of pancreatic ductal adenocarcinoma (PDAC) demonstrates that most tumors display a mixture of cells showing vastly different degrees of oncogenic KRAS dependency. We identify populations of cells that vary in their gene expression patterns pertaining to the predicted level of KRAS dependency, cell growth, and differentiation within each tumor. We focused on two major variables: the degree of cancer cell proliferation and differentiation commitment. We determined each variable's significance for the growth and treatment in tumors in mice. The data suggest that neither the intensity of RAS/MAPK signaling nor the differentiation trajectory of tumor cells can be predictive of tumor growth or treatment resistance. The ability of cancer cells to reside in a

A

B

C

D

E

F

G

IHC: P-ERK

IHC: KI67

IHC: CDH1

H&E

H
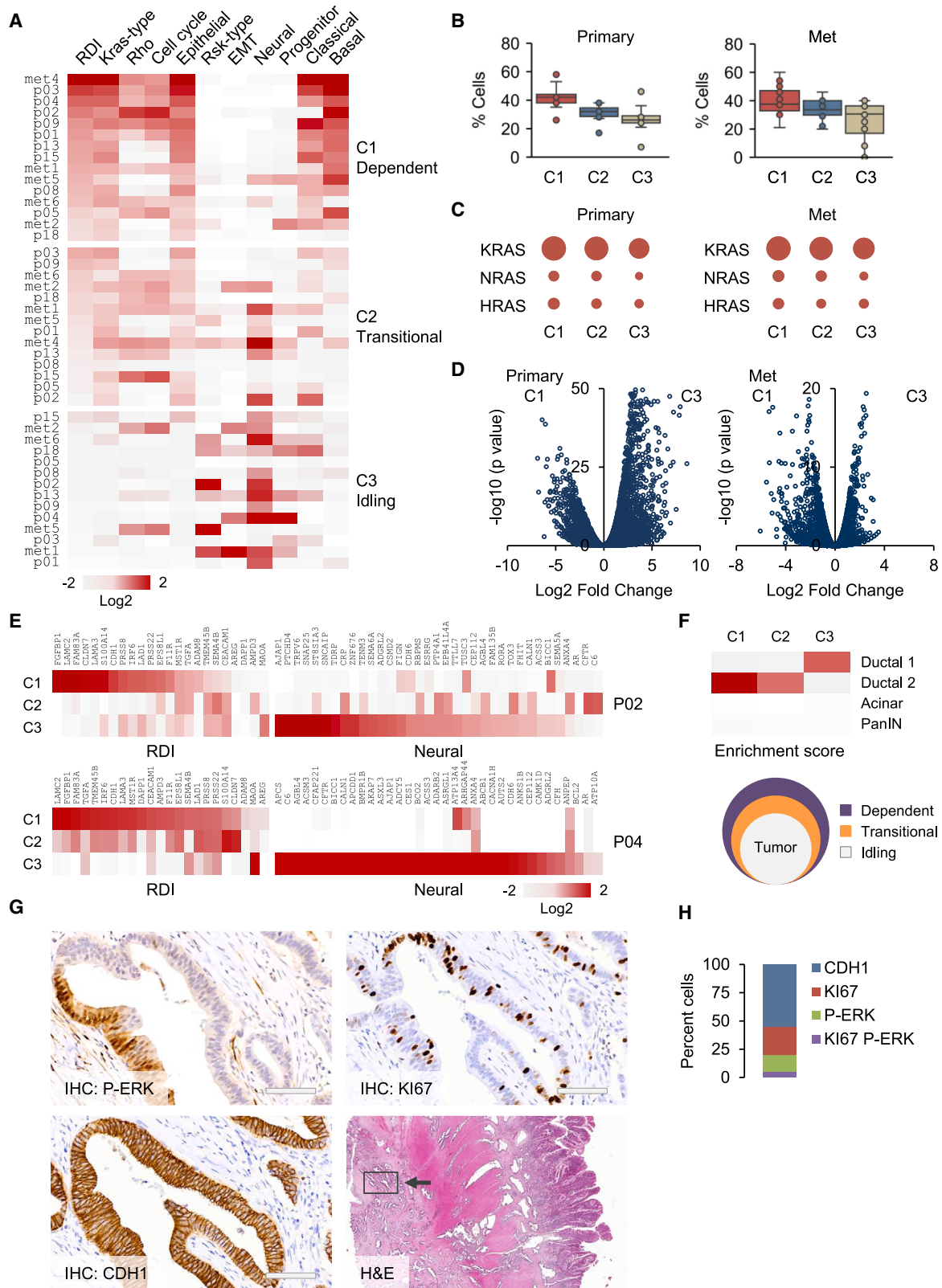
(legend on next page)

reversible quiescent state is an inherent property of KRAS-mutant tumors, necessitating alternative treatment strategies.

RESULTS

Single-cell sequencing of PDAC reveals recurring patterns of intratumor heterogeneity

We analyzed gene expression profiles of >200,000 single cells from three datasets (GSA: CRA001160, GSE154778, and GSE205013) that encompass over 20 primary and metastatic PDAC samples[19–21] (Table S1). Unsupervised clustering identified >10 cell subsets that were assigned to known cell types, including tumor cells, immune cells, cancer-associated fibroblasts, etc., using established marker genes.[21] Malignant cells within each tumor varied in their gene expression signatures pertaining to the predicted level of oncogenic KRAS dependency (RAS dependency indices [RDI]), cell cycle activation, and differentiation commitment. They segregated into three distinct clusters (termed C1, C2, and C3) exhibiting coherent gene expression patterns (Figures 1A and 1B). For cluster C1, we observed an enrichment of genes involved in oncogenic KRAS dependency,[15] RAS/MAPK signaling,[16] and epithelial differentiation[22] (Figure 1A; STAR Methods). Although MAPK is usually associated with proliferation, analysis revealed only a limited overlap between cell cycle genes (>200 genes involved in DNA replication and cell division) and MAPK pathway genes that mediate canonical RAS signaling.[16] Rather, there was a nearly perfect correspondence between cell cycle and signaling by RHO from the Reactome dataset (Pearson correlation coefficient $r > 0.9$, $p < 0.0001$). How such signaling heterogeneity arises between malignant cells in the same tumor is not understood and requires further study, as KRAS mRNA expression remained unperturbed for all three clusters (Figure 1C). However, this is consistent with synergism between RAS and RHO signaling.[16,23] It also aligns with reports showing that ERK activation and epithelial differentiation depend on epidermal growth factor receptor (EGFR) signaling activity, and hence on exogenous factors, rather than KRAS alone.[24,25] On a similar note, the consensus PDAC subtypes termed classical and basal overlapped in C1. However, gene expression changes in clusters C2 and C3 virtually silenced the basal-like expression program in the majority of samples (Figures 1A and S1A). It follows that the subtype differences do not generalize across tumors, but rather reflect their spatial organization.

On balance, cluster C1 had the highest expression of RAS target genes involved in epithelial differentiation (e.g., CDH1, EPCAM, CEACAMs, and CLDN family), as compared to the other cell populations. In all cases, MAPK3/ERK1 but not MAPK1/ERK2 expression was correlated strongly with higher RDI scores (Pearson's $r > 0.8$), suggesting that ERK activity is regulated by transcriptional mechanisms. Tumor cells in cluster C2 showed moderate changes in gene expression relative to C1 ($\geq$4-fold), while those in cluster C3 exhibited major gene expression shifts ($\geq$10-fold) (Figure 1D). Two features of cells in C3 stood out in particular: they did not carry features of the squamous or classical subtypes of PDAC (Figure 1A); they were marked by the gain of mesenchymal genes (CDH2, FN1, and VIM) or the recently characterized neural-like progenitor (NRP) genes (e.g., ASCL1, NRCAM, RELN, and SEMA family),[19,22,26] but clustered separately from non-tumor cells or precancerous lesions (Figures 1E and 1F). Reduced proliferation and increased infiltration of TILs (tumor-infiltrating lymphocytes) were the salient features of tumors with high NRP scores ($p < 0.001$) (Figure S1B). We therefore classified C3 cells as idling according to previous annotations.[27] Together, this suggests that most pancreatic tumors display a mixture of cells showing strong KRAS dependency and those that are more KRAS independent. This is consistent with a model of partially overlapping, yet distinct gene expression programs coexisting in individual PDACs, i.e., classical, transitional, and neural progenitor type.[22,28]

Immunohistochemistry (IHC) staining of tumor specimens obtained from over 20 patients with primary and metastatic PDAC confirmed an extensive heterogeneity in phosphorylation patterns of ERK and non-overlapping patterns of KI67 expression, a marker of cell proliferation ($p < 0.001$) (Figures 1G, 1H, and S1C). To support these observations, we examined pancreatic cell lines from the Cancer Cell Line Encyclopedia ($N = 49$). In addition to RAS/MAPK dependency scores,[15,16,29] we used curated gene sets derived from single-nucleus profiling of pancreatic cancer,[22] all giving highly concordant results. This analysis did not reveal any significant association between MAPK pathway activity and the cell cycle genes, although a strong positive correlation (co-expression) of the cell cycle genes with E2F and MYC-mediated transcription was observed for all cell lines tested (Pearson's $r > 0.8$) (Figure S1D). Although the heterogeneity of cancer cell lines is coupled with large random variation, the results are consistent with the differential sensitivity of KRAS-mutant cancers to oncogene-targeted therapy.[16]

KRAS inhibition uncouples MAPK signaling from cell cycle progression

Through analysis of single-cell data of mouse PDAC, we uncovered a high degree of intratumor heterogeneity and three cell

---

Figure 1. Single-cell sequencing of human PDAC reveals recurring patterns of intratumor heterogeneity in KRAS signaling

(A) Tumor cells from primary and metastatic PDAC samples ($N = 23$) were grouped into RAS-dependent (C1), transitional (C2), and idling (C3) using K-Means clustering algorithm. Average RAS dependency indices (RDI), ribosomal S6 kinase A (RSK), and epithelial-mesenchymal transition scores (EMT) are shown.

(B) Boxplots showing the distribution of different clusters in primary and metastatic tumors. Boxplots show center line as median, box limits as upper and lower quartiles, and whiskers represent a 1.5× interquartile range.

(C) Average expression of RAS family genes in scRNA sequencing data. The size of each bubble indicates average expression.

(D) Volcano plots showing the statistical significance of differentially expressed genes in clusters C1 and C3 relative to their magnitude. Primary (P04) and metastatic tumors (P02) are shown.

(E) Heatmaps depicting gene expression changes of individual genes in clusters C2 and C3. Primary (P04) and metastatic (P02) tumors are shown.

(F) Pathway enrichment analysis of tumor clusters focusing on C1, C2, and C3. Schematic diagram of data is shown.

(G) IHC staining results obtained with CDH1, P-ERK, and KI67 antibodies. Representative tumor is shown. Scale bar 100 μm.

(H) Quantitation of data shown in (G). Single-positive (CDH1, KI67, and P-ERK) and double-positive cells (KI67 and P-ERK) are shown.
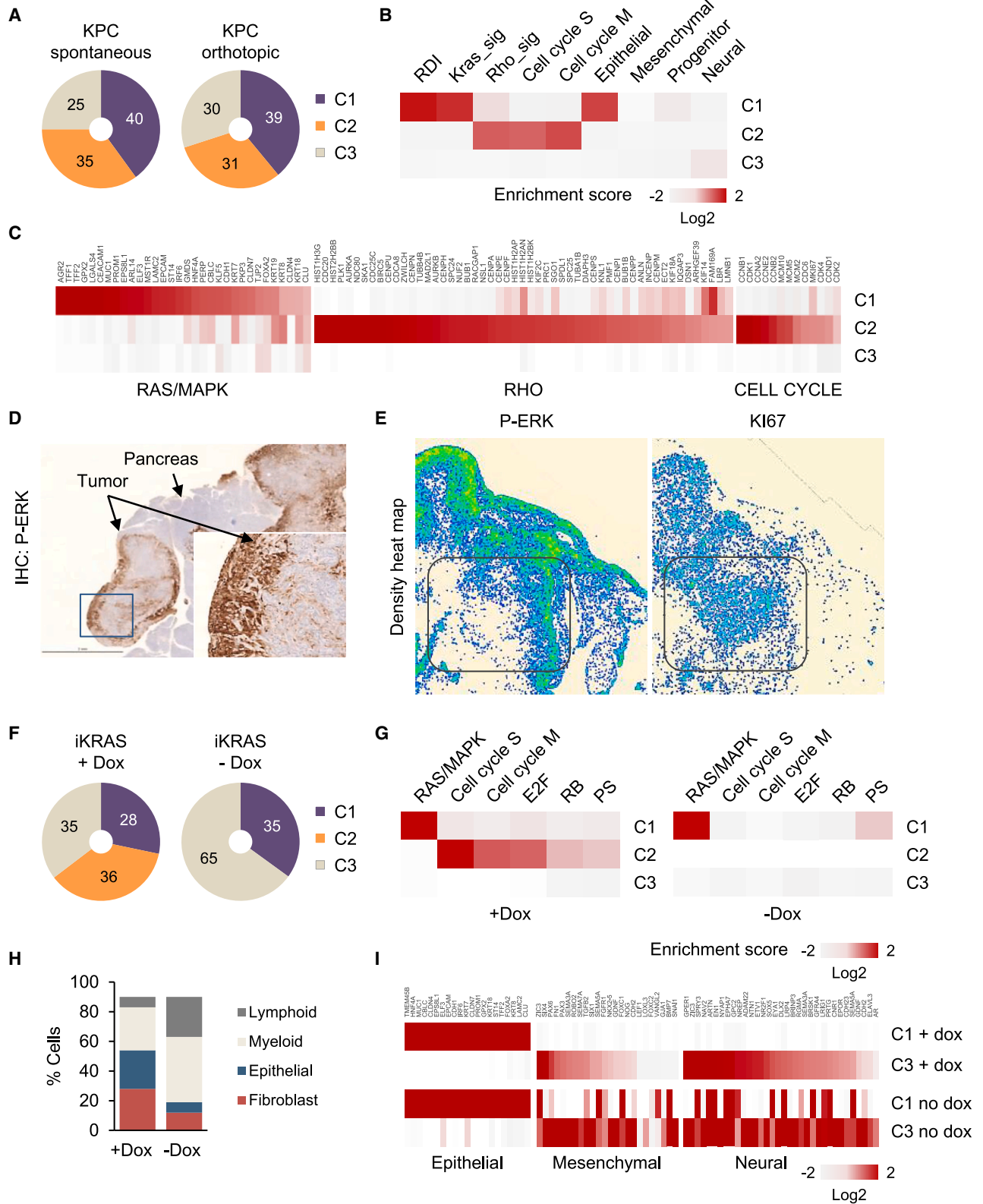
populations (C1, C2, and C3) with the aforementioned characteristics of human malignancies (Figure 2A; STAR Methods). Both spontaneous and transplantable models were examined (Table S1).[30–32] The KRAS dependency scores showed strong positive correlation with MAPK/ERK activation, while the expression of cell cycle genes clearly aligned with signaling by RHO (Figures 2B and 2C). It is worth noting that RAC1, a member of the RHO family, is an essential KRAS dependency gene whose genetic ablation prevents tumor development in mice.[33,34] Orthogonal validation of single-cell data by IHC showed that elevated phosphorylation of ERK or its downstream target S6 was confined to the tumor periphery (Figures 2D and S2A). However, we did not find a strong correlation of P-ERK staining with KI67 expression (Figures 2E and S2B). Numerically, about 40% of tumor cells belonged to cluster C1 with high average expression of genes involved in epithelial differentiation (exemplified by transcription factors ELF3, FOXA1/2, and HNF4A), whereas cells in C2 were less well differentiated and fully committed to cell cycle progression (Figures 2B and S2C). Cluster C3 was characterized by enrichment of mesenchymal over epithelial genes and partially overlapping expression patterns with KRAS knockouts ($p < 0.0001$), suggesting the minimum level of KRAS signaling activity (Figure S2D). To evaluate the tumorigenic potential of C3 cells relative to other cell populations, we generated KPC tumors expressing yellow fluorescent protein (YFP). The YFP tumor cells were then sorted by fluorescence-activated cell sorting (FACS) into three groups: EpCAM^{hi}CDH1^{hi} (corresponding to cluster C1), EpCAM^{lo}CDH1^{lo} (C2), and EpCAM^{neg}CDH1^{neg} (C3). Orthotopic transplantations into mice showed 100% penetrance of tumor formation by each FACS-sorted group. Thus, each cluster can govern latent relapse (Figure S2E).

To assess the impact of oncogenic KRAS on the survival versus proliferation of tumor cells, we used a doxycycline-inducible mouse model (termed iKRAS), in which administration of doxycycline leads to expression of KRAS^{G12D} and withdrawal of the drug inactivates its expression.[35] Because inactivation of MAPK genes suppresses KRAS-driven tumors,[36] we sought to mitigate the impact of KRAS/MAPK signaling through doxycycline withdrawal. Previous studies have shown that doxycycline withdrawal leads to tumor regression, with the time to complete regression ranging from 3 to 4 weeks.[35,37] We performed single-cell sequencing of iKRAS tumors grown in the presence of doxycycline or maintained in its absence for 4 days (see STAR Methods). Data analysis revealed that silencing KRAS^{G12D} wiped out the proliferative cluster C2, while sparing C1 and C3

(Figures 2F and 2G). We observed sustained activation of the top ranking MAPK target genes (e.g., FOS and JUN) and epithelial cell markers (CDH1, EPCAM, and KRT7/8). These genes exhibited highly consistent expression levels despite a 60% reduction in tumor size (Figure 2H), or the transition from proliferation to mixed-lineage differentiation (Figure 2I). Gene Ontology classification of biological processes showed an enrichment of pathways involved in cell-to-cell signaling and neurogenesis (Figure S3A). In situ analysis revealed persistent ERK phosphorylation throughout 2 weeks of doxycycline withdrawal (i.e., KRAS^{G12D} inactivation) (Figure S3B), corroborating previously published data on KRAS knockouts.[32,38] In summary, silencing KRAS does not alleviate MAPK activation but does uncouple it from cell cycle progression. The prolonged survival of C1 and C3 cells upon KRAS inactivation could be attributed, at least in part, to the repression of cell cycle genes and entry into a state of quiescence. This is exemplified by the reduction in DNA replication (E2F target genes), ribosome biogenesis, and protein translation (MYC target genes) observed in cluster C3 (Figure 2G). Since the parental cells used in this study were clonally derived, the C1, C2, and C3 tumor cell populations were isogenic. The ability of these cells to reversibly change between proliferation and quiescence may render them resistant to therapies that target KRAS.

The immune landscape of human PDAC

Immune cell profiling of iKRAS tumors identified discrete TIL populations whose expression profiles matched well with a reference list of marker genes.[39] Tumors with active KRAS expression were characterized by the presence of exhausted/dysfunctional CD8 T cells (PDCD1-high, GZMB-high, and HAVCR2-high), while tumors withdrawn from doxycycline were enriched in effector memory CD8 T cells (CD28-high, GZMB-high, and HAVCR2-high) and precursor-exhausted CD8 T cells (TCF7-high, GZMB-low, and HAVCR2-low) (Figure S4A). The population of precursor-exhausted CD8 T cells lacks high cytotoxic activity but seeds development of cytotoxic T lymphocytes.[40,41] Both CD4 and CD8 T cells expressed the inhibitory receptors PDCD1, CTLA4, LAG3, and HAVCR2 regardless of KRAS expression status (Figure S4A). This supports the notion that treatment of PDAC will require inhibition of KRAS and concurrent activation of immune pathways suppressed by cancer.[32,42]

To assess the reliability and robustness of single cell-clustering, we examined the gene expression profiles of over 300

Figure 2. KRAS inhibition uncouples MAPK signaling from cell cycle progression

(A) Tumor cells from spontaneous and orthotopic mouse PDAC samples ($N = 8$) were grouped into RAS-dependent (C1), transitional (C2), and idling (C3) using K-means clustering. The percentages of cells in each group are shown.

(B) Pathway enrichment analysis of tumor cells in clusters C1, C2, and C3.

(C) Heatmap depicting differential gene expression in clusters C1, C2, and C3.

(D) IHC staining of orthotopic KPC tumor obtained with P-ERK antibodies. Scale bar 2 mm.

(E) Density heatmaps of P-ERK and KI67 staining in an orthotopic KPC tumor.

(F) KRAS-inducible mouse PDACs (iKRAS model) were grouped according to gene expression signatures that segregate them into C1, C2, and C3 cell populations. Mice were treated with doxycycline for 3 weeks followed by withdrawal of doxycycline for 4 days.

(G) Gene expression differences in iKRAS tumors upon doxycycline withdrawal. Abbreviations: E2F, E2 transcription factors; PS, protein synthesis; RB, ribosome biogenesis.

(H) Relative proportions of tumor cells shown in (F).

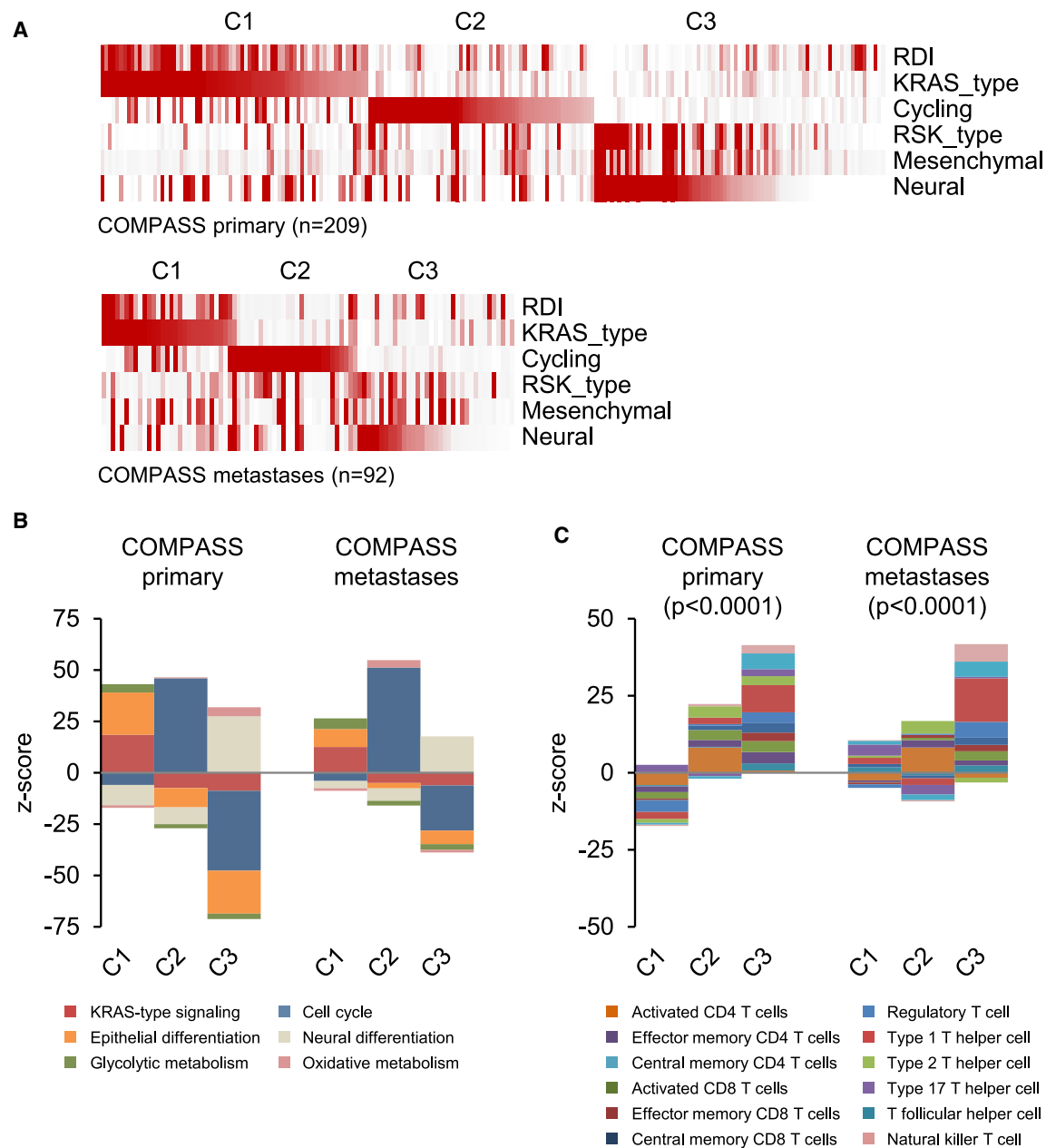(I) Expression of epithelial, mesenchymal, and neural genes in iKRAS tumors.

Figure 3. The immune landscape of human PDAC
(A) Distribution of primary and metastatic PDAC samples in the COMPASS dataset (N = 301).
(B) Pathway activity scores in primary and metastatic PDAC from the COMPASS dataset.
(C) TIL scores of C1, C2, and C3 tumors from the COMPASS dataset generated using gene expression data.

samples from the COMPASS database representing locally advanced and metastatic human PDAC.[43] Both primary (N = 209) and metastatic tumors (N = 92) were examined (Figure 3A). These tumors again fell into three groups (C1–C3) with high/low KRAS signaling activity (Figure 3A). Differentiation commitment, cell division, and the level of tumor immune infiltration were the most divergent phenotypic features across tumor types (Figures 3B and 3C). Sustained activation of the RAS/MAPK

pathway (tumors C1) was associated with low TIL scores and elevated expression of T cell dysfunction genes (CTLA4, HAVCR2, LAG3, PDCD1, and TIGIT) (Figures 3C and S4B). Tumors C2 displayed distinct characteristics that allow them to integrate E2F and MYC signaling outputs with low TIL infiltration (Figure 3C). In contrast, low KRAS dependency scores in tumor C3 were associated with enhanced TIL infiltration (p < 0.0001) dominated by type 1 helper, T regulatory, and natural killer

T cells (Figure 3C). Considering that KRAS mutations were evenly distributed throughout samples (90% in primary tumors; 89% in metastases), these data underscore the heterogeneity of KRAS signaling outputs within and across tumors.[43] To identify changes that correlated with cancer treatment, we examined the gene expression profiles of treatment-naive PDAC (The Cancer Genome Atlas, n = 150). These samples also fell into three categories with high/low KRAS signaling activity, supporting the concept of differential KRAS dependency (Figure S4C). High TIL grade inversely correlated with RAS/MAPK activity scores both before and after treatment. Statistically, C3-enriched tumors were twice as likely to have high TIL scores (Figure S4D).

The impact of phenotypic heterogeneity on treatment resistance

To model the impact of KRAS mutations on therapeutic response, we used CRISPR to inactivate KRAS in human CFPAC1 (KRAS[G12V]) and PANC1 (KRAS[G12D]) PDAC cell lines. The CFPAC1 cell line is generally considered to be KRAS dependent, while the PANC1 cell line is often classified as KRAS independent. Notably, loss of KRAS did not suppress CFPAC1 and PANC1 cell proliferation in vitro or in nude mice, supporting the notion that at least some PDAC tumors may rely on second mutations that regulate cell survival and proliferation.[44] Differential gene expression analysis of KRAS knockout clones identified genes that fell into three main groups based on their function: cell adhesion, cell differentiation, and neurogenesis (false discovery rate < 0.05) (Figures S5A and S5B). Previous studies reported a panel of KRAS-ablated PDAC cell lines, all showing highly divergent gene expression programs.[38,45] Among the processes enriched in KRAS-intact cells are cell adhesion, differentiation, and ribosomal biogenesis, whereas the gene expression profiles of KRAS-ablated cells are correlated with loss of epithelial commitment and extracellular matrix organization.[38,45]

To rationalize this phenotypic flexibility, we used inhibitors targeting KRAS (MRTX1133 and RMC-7977) along with its upstream regulators EGFR (erlotinib), SOS1 (BI-3406), SHP2 (SHP099), or downstream effectors MEK (trametinib [GSK1120212]), PI3K (alpelisib), and AKT (capivasertib). MRTX1133 targets KRAS[G12D], while RMC-7977 inhibits all GTP-bound RAS isoforms.[46,47] Because RHO proteins lack effective inhibitors, we targeted CDK4/6 (abemaciclib), with or without immune checkpoint inhibitors (ICIs). Our reasons were severalfold: vertical pathway inhibition (e.g., KRAS/MEK) improves the efficacy of RAS-targeted therapies[48]; oncogenic KRAS addiction is most strongly manifested in mice with an intact immune system[32]; and combination immunotherapy with KRAS/MEK inhibitors induces complete regression of pancreatic tumors in mice at 60%–80% efficiency.[18]

To evaluate the efficacy of these inhibitors, C57BL/6J mice bearing KPCY tumors (~6 mm diameter) were treated with vehicle or drug solutions for 6 days. Mice treated with the KRAS or pan-RAS inhibitor alone were not significantly affected. Dual inhibition of KRAS with EGFR, SHP2, SOS1, or CDK4 resulted in a modest reduction of tumor growth, while dual inhibition of KRAS/MEK caused partial regression (~40% reduction in tumor size) (Figure 4A). IHC staining of tumor sections confirmed that anti-RAS drugs failed to achieve adequate suppression of

ERK phosphorylation and KI67 expression (Figure 4B).[49] MEK inhibition was significantly more effective, as it reduced ERK phosphorylation, while maintaining CD8 T cell infiltration (Figures 4B and 4C). To evaluate whether synergistic efficacy can be achieved by combining anti-RAS drugs with ICIs, mice were treated with antibodies targeting CTLA4, PDCD1, and CD40.[50,51] Treatment with ICIs enhanced the anti-tumor effect of KRAS/MEK inhibition (≥70% reduction in tumor size) (Figures 4A and 4D). In comparison, targeting pan-RAS (RMC-7977), CDK4, EGFR, PI3K, SHP2, or SOS1 showed no meaningful regression, either in dual or triple combinations with ICIs (Figure 4A). Long-term use of these drugs over 14 days had a negligible effect on tumor regression, suggesting that their in vivo potency is low compared to cell-based assays.

Flow cytometry and IHC staining of samples using markers of tumor cells (CDH1, KI67, and YFP) and stromal cells (ACTA2 and THY1) revealed similar phenotypic changes occurring in KRAS-inhibited tumors and their KRAS-ablated counterparts, as there was a decrease of CDH1 and KI67 staining (clusters C1 and C2), and this was accompanied by the transition to high expression of YFP, implying an increase in fraction C3 (Figures S6A and S6B). Stromal markers were also increased about 2-fold compared with untreated controls (Figure S6A). This suggests strongly that pharmacological inhibition of KRAS can lead to phenotypic switching and, as a result, even the best KRAS inhibitors will have early resistance (shown schematically in Figure 4E). Moreover, examining the responses of individual KRAS-ablated cell lines revealed important differences with parental KRAS-intact cells. The most noticeable difference is that KRAS-ablated C1 cells tend to exhibit a more differentiated and therefore less aggressive phenotype (Figure 4F), whereas KRAS-ablated C3 cells are driven toward a poorly differentiated and potentially more aggressive phenotype, either acute or chronic (Figure 4G). This also increases the risk of RAS-independent tumor recurrence.[7,32] On the flip side, KRAS inactivation reverses immune evasion and renders tumors curable even within a short course of immunotherapy.

DISCUSSION

We used single-cell sequencing data of PDAC to show that KRAS signaling heterogeneity is not limited to tumors in different patients, but extends to tumors in the same patient. We stratified tumor cells based on KRAS dependency differences, cell growth, and differentiation commitment within each tumor. Although it is generally accepted that oncogene-addicted cancers, including KRAS-mutant cancers, are addicted to or dependent on RAS/MAPK signaling activity, our data suggest that virtually all pancreatic tumors contain a repertoire of cells showing reduced RAS/MAPK signaling. The KRAS dependency scores distinguishing different RAS/MAPK signaling states are broadly, and perhaps spatially, distributed across tumors, limiting their practical application. By the same token, the basal-like/classical subtype differences do not generalize across tumors but rather reflect their spatial distribution. While previous strategies to block KRAS therapeutically have focused mainly on counteracting its growth-promoting activity, we find that targeting of mutant KRAS suppresses growth of tumor cells with high
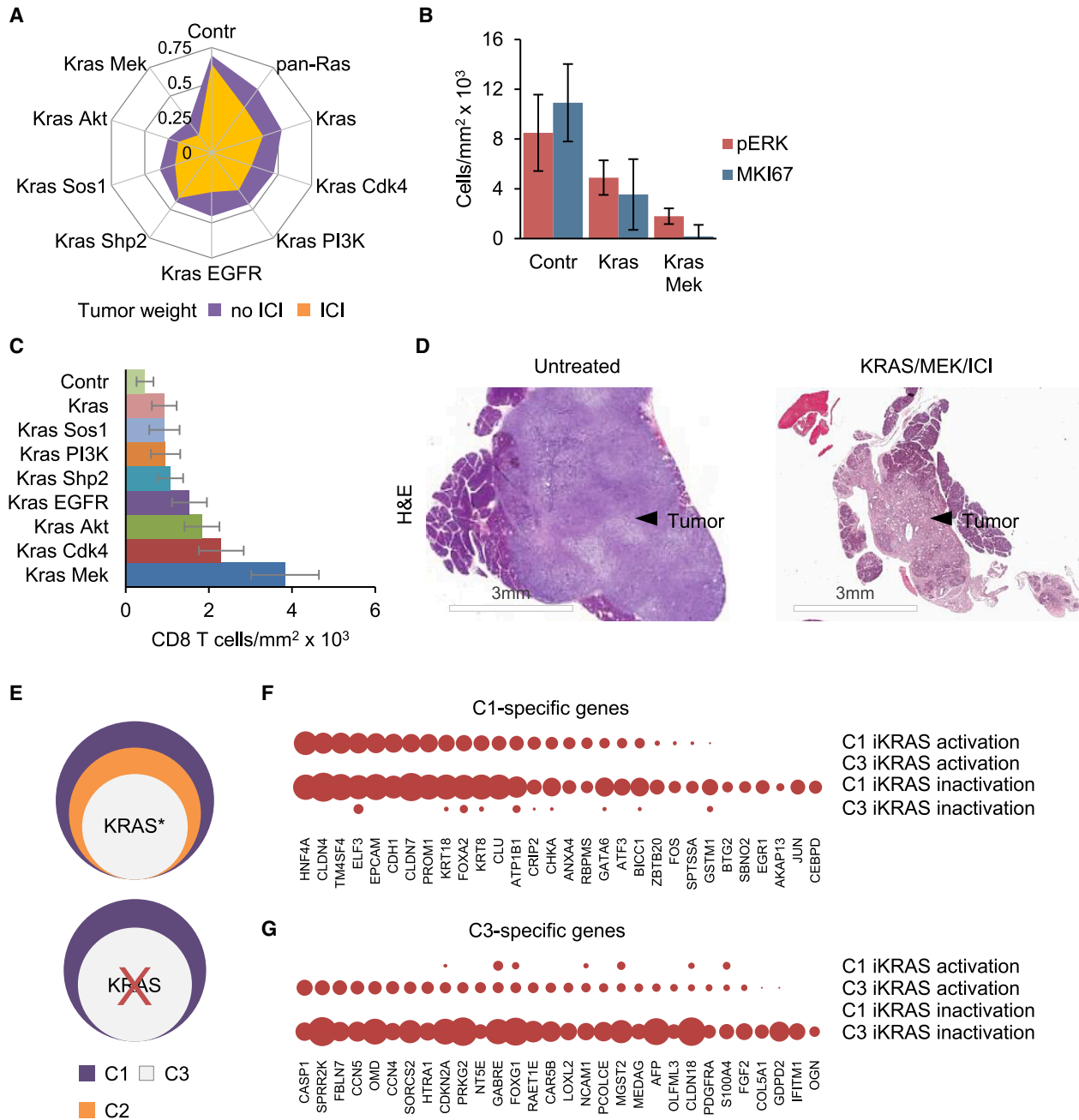
Figure 4. Phenotypic heterogeneity of tumor cells shapes treatment resistance

(A) Radar chart showing regression of KPCY tumors in C57BL6 mice treated with the indicated inhibitors and immune checkpoint inhibitors (ICIs) for 6 days ($n = 3$ per group).

(B) Frequency of P-ERK and KI67-positive cells in drug-treated tumors shown in (A). Data are represented as mean ± SEM.

(C) CD8 T cell infiltration in drug-treated tumors shown in (A). Data are represented as mean ± SEM.

(D) H&E staining of KPCY tumors shown in (A).

(E) KRAS-inactivated cells adopt the phenotypic properties of C1 and C3 cells.

(F and G) KRAS-inactivated tumor cells (iKRAS model) adopt the transcriptional properties of C1 and C3 cells.

RAS/MAPK signaling activity while sparing pre-existing subsets with low RAS signaling activity. Phenotype switching and acquisition of resistance are inextricably linked, representing the fundamental characteristic of KRAS-mutant tumors. Notably, the heterogeneity of cell states exists in mouse and human lung adenocarcinomas and arises independently of genetic

variation, consistent with the emergence of different cell identity programs.[52,53] On a cautionary note, the non-genetic cell state changes were found to correlate with tumor size. Samples having less than 200 tumor cells did not stratify well into dependent and independent and were excluded from analysis. Therefore, our stratification scheme may not fit all tumors sizes.

Despite a large number of PDAC subtype models that have been proposed, the extensive heterogeneity in KRAS signaling within and across tumors remains poorly explained.[54,55] The concept of KRAS dependency originally introduced as a measure of oncogenic addiction following KRAS inactivation has proven to be more multifaceted as it captures the diversity of cancer cell phenotypes within individual tumors. From a heterogeneity perspective, this study provides insights on how tumor cells regulate survival downstream of KRAS by switching to a hypo-proliferative state. Traditionally, the spotlight has been on the RAS/MAPK pathway, even though KRAS activates multiple pathways and the mutational status of KRAS is poorly correlated with the levels of ERK activation *in vivo*.[56–58] Moreover, KRAS knockout tumors display persistent ERK activation, calling into question the MAPK-centric paradigm of RAS tumorigenesis.[18,38] In fact, our data suggest that cell proliferation and ERK activation show an inverse relationship. Several issues remained unresolved. For instance, the question of whether or not there is a universal set of conditions required for KRAS-driven tumorigenesis. Or does a threshold exist for KRAS activation to block tumor growth? Indeed, KRAS is recurrently mutated only in some cancer types and not others. Furthermore, genetic ablation of mutant KRAS in mouse models of lung and pancreatic cancer causes complete tumor regression, whereas pharmacological inhibition using KRAS-blocking drugs delays but does not prevent tumor formation and growth.[14,32,46,47] Additionally, a common theme among tumors harboring mutant KRAS is their propensity to acquire secondary mutations that can affect cell survival and growth, and thereby limit the efficacy of targeted therapies. For instance, human PDAC cell lines from CCLE contain an average of over 20 cancer-related mutations and widespread copy-number gains.[59] Unlike human PDAC, mouse KPC tumors are dominated by copy-number alterations, while protein-altering mutations are rare.[60] Collectively, this provides a strong rationale for combining KRAS inhibitors with immune checkpoint inhibitors. Uncovering the mechanisms by which KRAS subverts T cell function is the key to successful treatment.

Limitations of the study

We are attempting to understand the ability of cancer cells to cycle between proliferation and quiescence by modeling human PDAC in the mouse, where the complexity of tumor cell types is not identical to that found in humans.

RESOURCE AVAILABILITY

Lead contact

Further information and requests for resources and reagents should be directed to and will be fulfilled by the lead contact, Nancy C. Reich (nancy.reich@stonybrook.edu).

Materials availability

This study did not generate any new reagents.

Data and code availability

- RNA sequencing data are deposited at Gene Expression Omnibus and Dryad repositories and are publicly available as of the date of publication.
- Accession numbers and codes are listed in the key resources table.
- The remaining data and information are available within the main text or supplementary materials, or available from the authors upon request. No restrictions on data availability such as a materials transfer agreement will be required.

AUTHOR CONTRIBUTIONS

O.P. designed the research; S.D. and O.P. performed the research; V.K. and O.P. contributed new reagents/analytic tools; O.P. and N.C.R. analyzed the data; and O.P. wrote the paper.

DECLARATION OF INTERESTS

The authors declare no competing interests.

STAR★METHODS

Detailed methods are provided in the online version of this paper and include the following:

- KEY RESOURCES TABLE
- EXPERIMENTAL MODEL AND STUDY PARTICIPANT DETAILS
  ○ Cell lines and culture conditions
  ○ *In vivo* animal studies
- METHOD DETAILS
- QUANTIFICATION AND STATISTICAL ANALYSIS

SUPPLEMENTAL INFORMATION

Supplemental information can be found online at https://doi.org/10.1016/j.isci.2024.111662.

REFERENCES

1. Awad, M.M., Liu, S., Rybkin, I.I., Arbour, K.C., Dilly, J., Zhu, V.W., Johnson, M.L., Heist, R.S., Patil, T., Riely, G.J., et al. (2021). Acquired resistance to KRASG12C inhibition in cancer. N. Engl. J. Med. *384*, 2382–2393. https://doi.org/10.1056/NEJMoa2105281.

2. Zhao, Y., Murciano-Goroff, Y.R., Xue, J.Y., Ang, A., Lucas, J., Mai, T.T., Da Cruz Paula, A.F., Saiki, A.Y., Mohn, D., Achanta, P., et al. (2021). Diverse alterations associated with resistance to KRAS(G12C) inhibition. Nature *599*, 679–683. https://doi.org/10.1038/s41586-021-04065-2.

3. Negrao, M.V., Araujo, H.A., Lamberti, G., Cooper, A.J., Akhave, N.S., Zhou, T., Delasos, L., Hicks, J.K., Aldea, M., Minuti, G., et al. (2023).

Comutations and KRASG12C Inhibitor Efficacy in Advanced NSCLC. Cancer Discov. 13, 1556–1571. https://doi.org/10.1158/2159-8290.CD-22-1420.

4. Yaeger, R., Mezzadra, R., Sinopoli, J., Bian, Y., Marasco, M., Kaplun, E., Gao, Y., Zhao, H., Paula, A.D.C., Zhu, Y., et al. (2023). Molecular Characterization of Acquired Resistance to KRASG12C-EGFR Inhibition in Colorectal Cancer. Cancer Discov. 13, 41–55. https://doi.org/10.1158/2159-8290.CD-22-0405.

5. Reiter, J.G., Baretti, M., Gerold, J.M., Makohon-Moore, A.P., Daud, A., Iacobuzio-Donahue, C.A., Azad, N.S., Kinzler, K.W., Nowak, M.A., and Vogelstein, B. (2019). An analysis of genetic heterogeneity in untreated cancers. Nat. Rev. Cancer 19, 639–650. https://doi.org/10.1038/s41568-019-0185-x.

6. Kapoor, A., Yao, W., Ying, H., Hua, S., Liewen, A., Wang, Q., Zhong, Y., Wu, C.J., Sadanandam, A., Hu, B., et al. (2014). Yap1 activation enables bypass of oncogenic Kras addiction in pancreatic cancer. Cell 158, 185–197. https://doi.org/10.1016/j.cell.2014.06.003.

7. Genovese, G., Carugo, A., Tepper, J., Robinson, F.S., Li, L., Svelto, M., Nezi, L., Corti, D., Minelli, R., Pettazzoni, P., et al. (2017). Synthetic vulnerabilities of mesenchymal subpopulations in pancreatic cancer. Nature 542, 362–366. https://doi.org/10.1038/nature21064.

8. Hou, P., Kapoor, A., Zhang, Q., Li, J., Wu, C.J., Li, J., Lan, Z., Tang, M., Ma, X., Ackroyd, J.J., et al. (2020). Tumor Microenvironment Remodeling Enables Bypass of Oncogenic KRAS Dependency in Pancreatic Cancer. Cancer Discov. 10, 1058–1077. https://doi.org/10.1158/2159-8290.CD-19-0597.

9. Tsai, Y.S., Woodcock, M.G., Azam, S.H., Thorne, L.B., Kanchi, K.L., Parker, J.S., Vincent, B.G., and Pecot, C.V. (2022). Rapid idiosyncratic mechanisms of clinical resistance to KRAS G12C inhibition. J. Clin. Invest. 132, e155523. https://doi.org/10.1172/JCI155523.

10. Tanaka, N., Lin, J.J., Li, C., Ryan, M.B., Zhang, J., Kiedrowski, L.A., Michel, A.G., Syed, M.U., Fella, K.A., Sakhi, M., et al. (2021). Clinical acquired resistance to KRASG12C inhibition through a novel KRAS switch-II pocket mutation and polyclonal alterations converging on RAS–MAPK reactivation. Cancer Discov. 11, 1913–1922. https://doi.org/10.1158/2159-8290.CD-21-0365.

11. Ryan, M.B., Coker, O., Sorokin, A., Fella, K., Barnes, H., Wong, E., Kanikarla, P., Gao, F., Zhang, Y., Zhou, L., et al. (2022). KRASG12C-independent feedback activation of wild-type RAS constrains KRASG12C inhibitor efficacy. Cell Rep. 39, 110993. https://doi.org/10.1016/j.celrep.2022.110993.

12. Adachi, Y., Kimura, R., Hirade, K., Yanase, S., Nishioka, Y., Kasuga, N., Yamaguchi, R., and Ebi, H. (2023). Scribble mis-localization induces adaptive resistance to KRAS G12C inhibitors through feedback activation of MAPK signaling mediated by YAP-induced MRAS. Nat. Can. (Ott.) 4, 829–843. https://doi.org/10.1038/s43018-023-00575-2.

13. Cannataro, V.L., Gaffney, S.G., Stender, C., Zhao, Z.M., Philips, M., Greenstein, A.E., and Townsend, J.P. (2018). Heterogeneity and mutation in KRAS and associated oncogenes: evaluating the potential for the evolution of resistance to targeting of KRAS G12C. Oncogene 37, 2444–2455. https://doi.org/10.1038/s41388-017-0105-z.

14. Salmón, M., Alvarez-Diaz, R., Fustero-Torre, C., Brehey, O., Lechuga, C.G., Sanclemente, M., Fernandez-Garcia, F., Lopez-Garcia, A., Martin-Guijarro, M.C., Rodriguez-Perales, S., et al. (2023). Kras oncogene ablation prevents resistance in advanced lung adenocarcinomas. J. Clin. Invest. 133, e164413. https://doi.org/10.1172/JCI164413.

15. Singh, A., Greninger, P., Rhodes, D., Koopman, L., Violette, S., Bardeesy, N., and Settleman, J. (2009). A gene expression signature associated with "K-Ras addiction" reveals regulators of EMT and tumor cell survival. Cancer Cell 15, 489–500. https://doi.org/10.1016/j.ccr.2009.03.022.

16. Yuan, T.L., Amzallag, A., Bagni, R., Yi, M., Afghani, S., Burgan, W., Fer, N., Strathern, L.A., Powell, K., Smith, B., et al. (2018). Differential Effector Engagement by Oncogenic KRAS. Cell Rep. 22, 1889–1902. https://doi.org/10.1016/j.celrep.2018.01.051.

17. Kelly, M.R., Kostyrko, K., Han, K., Mooney, N.A., Jeng, E.E., Spees, K., Dinh, P.T., Abbott, K.L., Gwinn, D.M., Sweet-Cordero, E.A., et al. (2020). Combined Proteomic and Genetic Interaction Mapping Reveals New RAS Effector Pathways and Susceptibilities. Cancer Discov. 10, 1950–1967. https://doi.org/10.1158/2159-8290.CD-19-1274.

18. Li, J., D'Amico, S., Kirillov, V., Petrenko, O., and Reich, N.C. (2023). Oncogenic dependency plays a dominant role in the immune response to cancer. Proc. Natl. Acad. Sci. USA 120, e2308635120. https://doi.org/10.1073/pnas.2308635120.

19. Peng, J., Sun, B.F., Chen, C.Y., Zhou, J.Y., Chen, Y.S., Chen, H., Liu, L., Huang, D., Jiang, J., Cui, G.S., et al. (2019). Single-cell RNA-seq highlights intra-tumoral heterogeneity and malignant progression in pancreatic ductal adenocarcinoma. Cell Res. 29, 725–738. https://doi.org/10.1038/s41422-019-0195-y.

20. Lin, W., Noel, P., Borazanci, E.H., Lee, J., Amini, A., Han, I.W., Heo, J.S., Jameson, G.S., Fraser, C., Steinbach, M., et al. (2020). Single-cell transcriptome analysis of tumor and stromal compartments of pancreatic ductal adenocarcinoma primary tumors and metastatic lesions. Genome Med. 12, 80. https://doi.org/10.1186/s13073-020-00776-9.

21. Werba, G., Weissinger, D., Kawaler, E.A., Zhao, E., Kalfakakou, D., Dhara, S., Wang, L., Lim, H.B., Oh, G., Jing, X., et al. (2023). Single-cell RNA sequencing reveals the effects of chemotherapy on human pancreatic adenocarcinoma and its tumor microenvironment. Nat. Commun. 14, 797. https://doi.org/10.1038/s41467-023-36296-4.

22. Hwang, W.L., Jagadeesh, K.A., Guo, J.A., Hoffman, H.I., Yadollahpour, P., Reeves, J.W., Mohan, R., Drokhlyansky, E., Van Wittenberghe, N., Ashenberg, O., et al. (2022). Single-nucleus and spatial transcriptome profiling of pancreatic cancer identifies multicellular dynamics associated with neoadjuvant treatment. Nat. Genet. 54, 1178–1191. https://doi.org/10.1038/s41588-022-01134-8.

23. Coleman, M.L., Marshall, C.J., and Olson, M.F. (2004). RAS and RHO GTPases in G1-phase cell-cycle regulation. Nat. Rev. Mol. Cell Biol. 5, 355–366. https://doi.org/10.1038/nrm1365.

24. Ardito, C.M., Grüner, B.M., Takeuchi, K.K., Lubeseder-Martellato, C., Teichmann, N., Mazur, P.K., Delgiorno, K.E., Carpenter, E.S., Halbrook, C.J., Hall, J.C., et al. (2012). EGF receptor is required for KRAS-induced pancreatic tumorigenesis. Cancer Cell 22, 304–317. https://doi.org/10.1016/j.ccr.2012.07.024.

25. Navas, C., Hernández-Porras, I., Schuhmacher, A.J., Sibilia, M., Guerra, C., and Barbacid, M. (2012). EGF receptor signaling is essential for k-ras oncogene-driven pancreatic ductal adenocarcinoma. Cancer Cell 22, 318–330. https://doi.org/10.1016/j.ccr.2012.08.001.

26. Zhang, L., Ma, J., Zhou, D., Zhou, J., Hu, B., Ma, X., Tang, J., Bai, Y., Chen, H., and Jing, Y. (2023). Single-Nucleus Transcriptome Profiling of Locally Advanced Cervical Squamous Cell Cancer Identifies Neural-Like Progenitor Program Associated with the Efficacy of Radiotherapy. Adv. Sci. 10, e2300348. https://doi.org/10.1002/advs.202300348.

27. Tosti, L., Hang, Y., Debnath, O., Tiesmeyer, S., Trefzer, T., Steiger, K., Ten, F.W., Lukassen, S., Ballke, S., Kühl, A.A., et al. (2021). Single-Nucleus and In Situ RNA-Sequencing Reveal Cell Topographies in the Human Pancreas. Gastroenterology 160, 1330–1344.e11. https://doi.org/10.1053/j.gastro.2020.11.010.

28. Di Chiaro, P., Nacci, L., Arco, F., Brandini, S., Polletti, S., Palamidessi, A., Donati, B., Soriani, C., Gualdrini, F., Frigè, G., et al. (2024). Mapping functional to morphological variation reveals the basis of regional extracellular matrix subversion and nerve invasion in pancreatic cancer. Cancer Cell 42, 662–681.e10. https://doi.org/10.1016/j.ccell.2024.02.017.

29. Janes, M.R., Zhang, J., Li, L.S., Hansen, R., Peters, U., Guo, X., Chen, Y., Babbar, A., Firdaus, S.J., Darjania, L., et al. (2018). Targeting KRAS Mutant Cancers with a Covalent G12C-Specific Inhibitor. Cell 172, 578–589.e17. https://doi.org/10.1016/j.cell.2018.01.006.

30. Elyada, E., Bolisetty, M., Laise, P., Flynn, W.F., Courtois, E.T., Burkhart, R.A., Teinor, J.A., Belleau, P., Biffi, G., Lucito, M.S., et al. (2019). Cross-Species Single-Cell Analysis of Pancreatic Ductal Adenocarcinoma

Reveals Antigen-Presenting Cancer-Associated Fibroblasts. Cancer Discov. *9*, 1102–1123. https://doi.org/10.1158/2159-8290.CD-19-0094.

31. Carstens, J.L., Yang, S., Correa de Sampaio, P., Zheng, X., Barua, S., McAndrews, K.M., Rao, A., Burks, J.K., Rhim, A.D., and Kalluri, R. (2021). Stabilized epithelial phenotype of cancer cells in primary tumors leads to increased colonization of liver metastasis in pancreatic cancer. Cell Rep. *35*, 108990. https://doi.org/10.1016/j.celrep.2021.108990.

32. Ischenko, I., D'Amico, S., Rao, M., Li, J., Hayman, M.J., Powers, S., Petrenko, O., and Reich, N.C. (2021). KRAS drives immune evasion in a genetic model of pancreatic cancer. Nat. Commun. *12*, 1482. https://doi.org/10.1038/s41467-021-21736-w.

33. Heid, I., Lubeseder-Martellato, C., Sipos, B., Mazur, P.K., Lesina, M., Schmid, R.M., and Siveke, J.T. (2011). Early requirement of Rac1 in a mouse model of pancreatic cancer. Gastroenterology *141*, 719–730. https://doi.org/10.1053/j.gastro.2011.04.043.

34. Wu, C.Y.C., Carpenter, E.S., Takeuchi, K.K., Halbrook, C.J., Peverley, L.V., Bien, H., Hall, J.C., DelGiorno, K.E., Pal, D., Song, Y., et al. (2014). PI3K regulation of RAC1 is required for KRAS-induced pancreatic tumorigenesis in mice. Gastroenterology *147*, 1405–1416.e7. https://doi.org/10.1053/j.gastro.2014.08.032.

35. Collins, M.A., Brisset, J.C., Zhang, Y., Bednar, F., Pierre, J., Heist, K.A., Galbán, C.J., Galbán, S., and di Magliano, M.P. (2012). Metastatic pancreatic cancer is dependent on oncogenic Kras in mice. PLoS One *7*, e49707. https://doi.org/10.1371/journal.pone.0049707.

36. Drosten, M., and Barbacid, M. (2020). Targeting the MAPK Pathway in KRAS-Driven Tumors. Cancer Cell *37*, 543–550. https://doi.org/10.1016/j.ccell.2020.03.013.

37. Fisher, G.H., Wellen, S.L., Klimstra, D., Lenczowski, J.M., Tichelaar, J.W., Lizak, M.J., Whitsett, J.A., Koretsky, A., and Varmus, H.E. (2001). Induction and apoptotic regression of lung adenocarcinomas by regulation of a K-Ras transgene in the presence and absence of tumor suppressor genes. Genes Dev. *15*, 3249–3262. https://doi.org/10.1101/gad.947701.

38. Muzumdar, M.D., Chen, P.Y., Dorans, K.J., Chung, K.M., Bhutkar, A., Hong, E., Noll, E.M., Sprick, M.R., Trumpp, A., and Jacks, T. (2017). Survival of pancreatic cancer cells lacking KRAS function. Nat. Commun. *8*, 1090. https://doi.org/10.1038/s41467-017-00942-5.

39. Andreatta, M., Corria-Osorio, J., Müller, S., Cubas, R., Coukos, G., and Carmona, S.J. (2021). Interpretation of T cell states from single-cell transcriptomics data using reference atlases. Nat. Commun. *12*, 2965. https://doi.org/10.1038/s41467-021-23324-4.

40. Chen, Z., Ji, Z., Ngiow, S.F., Manne, S., Cai, Z., Huang, A.C., Johnson, J., Staupe, R.P., Bengsch, B., Xu, C., et al. (2019). TCF-1-Centered Transcriptional Network Drives an Effector versus Exhausted CD8 T Cell-Fate Decision. Immunity *51*, 840–855.e5. https://doi.org/10.1016/j.immuni.2019.09.013.

41. Pais Ferreira, D., Silva, J.G., Wyss, T., Fuertes Marraco, S.A., Scarpellino, L., Charmoy, M., Maas, R., Siddiqui, I., Tang, L., Joyce, J.A., et al. (2020). Central memory CD8+ T cells derive from stem-like Tcf7hi effector cells in the absence of cytotoxic differentiation. Immunity *53*, 985–1000.e11. https://doi.org/10.1016/j.immuni.2020.09.005.

42. Wasko, U.N., Jiang, J., Dalton, T.C., Curiel-Garcia, A., Edwards, A.C., Wang, Y., Lee, B., Orlen, M., Tian, S., Stalnecker, C.A., et al. (2024). Tumour-selective activity of RAS-GTP inhibition in pancreatic cancer. Nature *629*, 927–936. https://doi.org/10.1038/s41586-024-07379-z.

43. Chan-Seng-Yue, M., Kim, J.C., Wilson, G.W., Ng, K., Figueroa, E.F., O'Kane, G.M., Connor, A.A., Denroche, R.E., Grant, R.C., McLeod, J., et al. (2020). Transcription phenotypes of pancreatic cancer are driven by genomic events during tumor evolution. Nat. Genet. *52*, 231–240. https://doi.org/10.1038/s41588-019-0566-9.

44. Hayashi, A., Hong, J., and Iacobuzio-Donahue, C.A. (2021). The pancreatic cancer genome revisited. Nat. Rev. Gastroenterol. Hepatol. *18*, 469–481. https://doi.org/10.1038/s41575-021-00463-z.

45. Lentsch, E., Li, L., Pfeffer, S., Ekici, A.B., Taher, L., Pilarsky, C., and Grützmann, R. (2019). CRISPR/Cas9-mediated knock-out of krasG12D mutated pancreatic cancer cell lines. Int. J. Mol. Sci. *20*, 5706. https://doi.org/10.3390/ijms20225706.

46. Kemp, S.B., Cheng, N., Markosyan, N., Sor, R., Kim, I.K., Hallin, J., Shoush, J., Quinones, L., Brown, N.V., Bassett, J.B., et al. (2023). Efficacy of a Small-Molecule Inhibitor of KrasG12D in Immunocompetent Models of Pancreatic Cancer. Cancer Discov. *13*, 298–311. https://doi.org/10.1158/2159-8290.CD-22-1066.

47. Holderfield, M., Lee, B.J., Jiang, J., Tomlinson, A., Seamon, K.J., Mira, A., Patrucco, E., Goodhart, G., Dilly, J., Gindin, Y., et al. (2024). Concurrent inhibition of oncogenic and wild-type RAS-GTP for cancer therapy. Nature *629*, 919–926. https://doi.org/10.1038/s41586-024-07205-6.

48. Molina-Arcas, M., and Downward, J. (2024). Exploiting the therapeutic implications of KRAS inhibition on tumor immunity. Cancer Cell *42*, 338–357. https://doi.org/10.1016/j.ccell.2024.02.012.

49. Singhal, A., Styers, H.C., Rub, J., Li, Z., Torborg, S.R., Kim, J.Y., Grbovic-Huezo, O., Feng, H., Tarcan, Z.C., Sahin Ozkan, H., et al. (2024). A Classical Epithelial State Drives Acute Resistance to KRAS Inhibition in Pancreatic Cancer. Cancer Discov. *14*, 2122–2134. https://doi.org/10.1158/2159-8290.CD-24-0740.

50. Morrison, A.H., Diamond, M.S., Hay, C.A., Byrne, K.T., and Vonderheide, R.H. (2020). Sufficiency of CD40 activation and immune checkpoint blockade for T cell priming and tumor immunity. Proc. Natl. Acad. Sci. USA *117*, 8022–8031. https://doi.org/10.1073/pnas.1918971117.

51. Freed-Pastor, W.A., Lambert, L.J., Ely, Z.A., Pattada, N.B., Bhutkar, A., Eng, G., Mercer, K.L., Garcia, A.P., Lin, L., Rideout, W.M., 3rd., et al. (2021). The CD155/TIGIT axis promotes and maintains immune evasion in neoantigen-expressing pancreatic cancer. Cancer Cell *39*, 1342–1360.e14. https://doi.org/10.1016/j.ccell.2021.07.007.

52. Marjanovic, N.D., Hofree, M., Chan, J.E., Canner, D., Wu, K., Trakala, M., Hartmann, G.G., Smith, O.C., Kim, J.Y., Evans, K.V., et al. (2020). Emergence of a High-Plasticity Cell State during Lung Cancer Evolution. Cancer Cell *38*, 229–246.e13. https://doi.org/10.1016/j.ccell.2020.06.012.

53. Han, G., Sinjab, A., Rahal, Z., Lynch, A.M., Treekitkarnmongkol, W., Liu, Y., Serrano, A.G., Feng, J., Liang, K., Khan, K., et al. (2024). An atlas of epithelial cell states and plasticity in lung adenocarcinoma. Nature *627*, 656–663. https://doi.org/10.1038/s41586-024-07113-9.

54. Collisson, E.A., Bailey, P., Chang, D.K., and Biankin, A.V. (2019). Molecular subtypes of pancreatic cancer. Nat. Rev. Gastroenterol. Hepatol. *16*, 207–220. https://doi.org/10.1038/s41575-019-0109-y.

55. Torre-Healy, L.A., Kawalerski, R.R., Oh, K., Chrastecka, L., Peng, X.L., Aguirre, A.J., Rashid, N.U., Yeh, J.J., and Moffitt, R.A. (2023). Open-source curation of a pancreatic ductal adenocarcinoma gene expression analysis platform (pdacR) supports a two-subtype model. Commun. Biol. *6*, 163. https://doi.org/10.1038/s42003-023-04461-6.

56. Cicchini, M., Buza, E.L., Sagal, K.M., Gudiel, A.A., Durham, A.C., and Feldser, D.M. (2017). Context-Dependent Effects of Amplified MAPK Signaling during Lung Adenocarcinoma Initiation and Progression. Cell Rep. *18*, 1958–1969. https://doi.org/10.1016/j.celrep.2017.01.069.

57. Poulin, E.J., Bera, A.K., Lu, J., Lin, Y.J., Strasser, S.D., Paulo, J.A., Huang, T.Q., Morales, C., Yan, W., Cook, J., et al. (2019). Tissue-specific oncogenic activity of KRASA146T. Cancer Discov. *9*, 738–755. https://doi.org/10.1158/2159-8290.CD-18-1220.

58. Zafra, M.P., Parsons, M.J., Kim, J., Alonso-Curbelo, D., Goswami, S., Schatoff, E.M., Han, T., Katti, A., Fernandez, M.T.C., Wilkinson, J.E., et al. (2020). An in vivo kras allelic series reveals distinct phenotypes of common oncogenic variants. Cancer Discov. *10*, 1654–1671. https://doi.org/10.1158/2159-8290.CD-20-0442.

59. Ghandi, M., Huang, F.W., Jané-Valbuena, J., Kryukov, G.V., Lo, C.C., McDonald, E.R., 3rd, Barretina, J., Gelfand, E.T., Bielski, C.M., Li, H., et al. (2019). Next-generation characterization of the Cancer Cell Line

Encyclopedia. Nature *569*, 503–508. https://doi.org/10.1038/s41586-019-1186-3.

60. Chung, W.J., Daemen, A., Cheng, J.H., Long, J.E., Cooper, J.E., Wang, B.E., Tran, C., Singh, M., Gnad, F., Modrusan, Z., et al. (2017). Kras mutant genetically engineered mouse models of human cancers are genomically heterogeneous. Proc. Natl. Acad. Sci. USA *114*, E10947–E10955. https://doi.org/10.1073/pnas.1708391114.

61. Hingorani, S.R., Wang, L., Multani, A.S., Combs, C., Deramaudt, T.B., Hruban, R.H., Rustgi, A.K., Chang, S., and Tuveson, D.A. (2005). Trp53R172H and KrasG12D cooperate to promote chromosomal instability and widely metastatic pancreatic ductal adenocarcinoma in mice. Cancer Cell *7*, 469–483. https://doi.org/10.1016/j.ccr.2005.04.023.

62. Li, J., Byrne, K.T., Yan, F., Yamazoe, T., Chen, Z., Baslan, T., Richman, L.P., Lin, J.H., Sun, Y.H., Rech, A.J., et al. (2018). Tumor Cell-Intrinsic Factors Underlie Heterogeneity of Immune Cell Infiltration and Response to Immunotherapy. Immunity *49*, 178–193.e7. https://doi.org/10.1016/j.immuni.2018.06.006.

STAR★METHODS

KEY RESOURCES TABLE

REAGENT or RESOURCE	SOURCE	IDENTIFIER
Antibodies		
Rabbit anti-KI67 antibody	Abcam	Cat# ab15580 RRID:AB_302459
Rabbit anti-alpha smooth muscle Actin antibody	Abcam	Clone 1A4 Catt# ab7817 RRID:AB_262054
Mouse ant-CDH1 antibody	Cell Signaling	Clone 4A2 Cat# 14472 RRID:AB_2728770
Rabbit anti-p44/42 MAPK (Erk1/2) antibody	Cell Signaling	Cat# 4695 RRID:AB_390779
Rabbit anti-Phospho-S6 Ribosomal Protein antibody	Cell Signaling	Cat# 4858 RRID:AB_916156
Rabbit anti-GFP antibody	Cell Signaling	Clone D5.1 Cat# 2956 RRID:AB_1196615
Rabbit anti-CD3 monoclonal antibody	Cell Signaling	Clone D8A8Y Cat# 85336
Rabbit anti-CD8a monoclonal antibody	Cell Signaling	Clone D8A8Y Cat# 85336
Rat anti-CD326 (EpCAM) monoclonal antibody (G8.8), APC	Invitrogen	Cat# 17-5791-82
APC Rat CD90.1 (Thy-1.1) monoclonal antibody (HIS51)	Invitrogen	Cat# 17-0900-82
PE Rat Anti-Mouse CD324 (E-Cadherin) monoclonal antibody	BD Biosciences	Cat# 567052
Anti-PD1 (BE0146)	BioXCell	Clone RMP1-14 Cat# BE0146
Anti-CTLA4 (BE0164)	BioXCell	Clone 9D9 Cat# BE0164
Anti-CD40 (BE0016)	BioXCell	Clone FGK4.5/FGK45 Cat# BE0016
Rat IgG2a	BioXCell	Clone 2A3 Cat# BE0089
Bacterial and virus strains		
DH5α Competent Cells	ThermoFisher	N/A
Biological samples		
Human pancreatic tissue blocks	Stony Brook BioBank	https://cancer.stonybrookmedicine.edu/research/biobank
Chemicals, peptides, and recombinant proteins		
MRTX1133	ChemieTek	Cat# CT-MTX1133
RMC-7977	ChemieTek	Cat# CT-RMC7977
Trametinib (GSK1120212)	Selleckchem	Cat# S2673
Abemaciclib	Selleckchem	Cat# S5716
Alpelisib	Selleckchem	Cat# S2814
BI-3406	Selleckchem	Cat# S8916
Capivasertib	Selleckchem	Cat# S8019
Erlotinib	Selleckchem	Cat# S7786
SHP099	Selleckchem	Cat# S6388
Gibco DMEM	Fisher Scientific	Cat# 10313039
Gibco Opti-MEM	Fisher Scientific	Cat# 11-058-021
Trypsin	Fisher Scientific	Cat# 25-200-056
Puromycin	Fisher Scientific	Cat# A1113803
Antibiotic-Antimycotic (100X)	Fisher Scientific	Cat# 15-240-112
Propidium Iodide Staining Solution	Fisher Scientific	Cat# 50-187-86
Corning Matrigel	Fisher Scientific	Cat# CB-40234A

(Continued on next page)

Continued

REAGENT or RESOURCE	SOURCE	IDENTIFIER
Taq DNA polymerase	Fisher Scientific	Cat# 10342053
Collagenase/Hyaluronidase	STEMCELL	Cat# 07912
DNase I	STEMCELL	Cat# 07900
Critical commercial assays		
Qiagen RNeasy Plus Mini kit	Fisher Scientific	ID: 73404
QiaAmp DNA Mini Kit	Fisher Scientific	ID: 51304
Single Cell 3′ Reagent Kit	10XGenomics	PN-120237
GenomePlex Single Cell Whole Genome Amplification Kit	Sigma	EC Number: 254-457-8
Deposited data		
Human: Single cell RNAseq	Peng et al.[19]	GSA: CRA001160
Human: Single cell RNAseq	Lin et al.[20]	GSE154778
Human: Single cell RNAseq	Werba et al.[21]	GSE205013
Human: PanCuRx PDAC	Chan-Seng-Yue et al.[43]	EGAS00001002543
Human: TCGA PDAC	PanCancer Atlas	www.cbioportal.org
Mouse: Single cell RNAseq	Elyada et al.[30]	GSE129455
Mouse: Single cell RNAseq	Carstens et al.[31]	GSE165534
Mouse: Single cell RNAseq	Ischenko et al.[32]	GSE132582
Mouse: Single cell RNAseq	This paper	GSE275858 security token qrkvommkvrevxat
Mouse: Bulk RNAseq	This paper	https://doi.org/10.5061/dryad.5hqbzkhct
Mouse: Bulk RNAseq	This paper	https://doi.org/10.5061/dryad.z8w9ghxks
Experimental models: Cell lines		
Human: PANC1	ATCC	CRL-1469
Human: CFPAC1	ATCC	CRL-1918
Mouse: A9312	Collins et al.[35]	N/A
Mouse: A9993	Collins et al.[35]	N/A
Mouse: FC1199	Hingorani et al.[61]	N/A
Mouse: 6419c5	Li et al.[62]	N/A
Experimental models: Organisms/strains		
C57BL/6J mice	The Jackson Laboratory	000664
FVB/NJ mice	The Jackson Laboratory	001800
Oligonucleotides		
PANC1 direct: gtagttggagctgatggcgt	This paper	N/A
PANC1 reverse: acgccatcagctccaactac	This paper	N/A
CFPAC1 direct: gtagttggagctgttggcgt	This paper	N/A
CFPAC1 reverse: acgccaacagctccaactac	This paper	N/A
Recombinant DNA		
lentiCRISPRv2 puro	Addgene	Plasmid #98290
Software and algorithms		
Cellranger (10XGenomics)	10XGenomics	v3.1.0
10xLoupe Browser	10XGenomics	V8
ShinyGO	http://bioinformatics.sdstate.edu/go/	V0.80
Other		
Sequence data, analyses, and resources related to RNA sequencing of KRAS knockout cells and matched normal	This paper	N/A

EXPERIMENTAL MODEL AND STUDY PARTICIPANT DETAILS

We analyzed gene expression profiles of human and mouse PDACs from publicly available datasets listed in key resources table.[19–21,30,31] K-means or graph-based clustering was used to divide cells into groups exhibiting relevant sets of co-expressed genes, biological pathways, and cell type assignments. The best number of clusters (k) was determined using the Elbow method. Pathway activity scores were determined using curated gene sets from the Molecular Signatures Database (Broad Institute). The activity score for each pathway was calculated as the mean expression level of all genes in this pathway. Heat maps and scatterplots were generated using the Excel software.

Cell lines and culture conditions

We analyzed KPC cell lines derived from KrasG12D; Trp53 R172H; Pdx1-Cre mice provided by Dr. David Tuveson (FC1199)[61] or KPC mice expressing the YFP lineage tag (KPCY) provided by Dr. Ben Stanger (6419c5),[62] and iKras cell lines (A9312 and A9993) derived from p48Cre; TetO-KrasG12D; Rosa26rtTa/+; p53R172H/+ mice provided by Dr. Marina Pasca di Magliano.[35] The CFPAC1 and PANC1 cell lines were purchased from ATCC. Cells were grown in DMEM supplemented with 5% FBS. The cell lines were routinely tested for mycoplasma contamination. For sgRNA sequences used in CRISPR/Cas9-mediated knockouts refer to the key resources table. Knockout efficiency was measured by Western blotting. Multiple technical replicates were obtained for each CRISPR-targeted cell line. Genomic DNA for PCR and Sanger sequencing was isolated using QiaAmp DNA Mini Kit (Qiagen). PCR products were amplified using Taq DNA polymerase (Invitrogen) and cloned into a pBluescript vector. At least 10 bacterial colonies were sequenced per cell line.

In vivo animal studies

All animal studies complied with relevant ethical regulations for animal testing and research and were approved by the Institutional Animal Care and Use Committee of Stony Brook University (protocol 2011-0356). We used C57BL/6J and FVB mice (The Jackson Laboratory). Experimentally naive male and female mice (8–10 week old) were housed individually for 2 weeks prior to surgery. Orthotopic injections into the pancreas were performed using 10^4 cells in 100 μL of Matrigel (Corning) diluted 1:7 with Opti-MEM (Gibco). The animals were observed for tumor development by palpation. The endpoint was tumor volume of ∼360 mm^3 (9 mm diameter). A total of 60 mice were randomly divided into treatment groups defined according to the experimental conditions. MRTX1133 and RMC-7977 (ChemieTek) were administered on days 1, 3, and 5 of treatment via IP injection at 10 mg/kg/day. Abemaciclib, Alpelisib, BI-3406, Capivasertib, Erlotinib, and SHP099 (Selleckchem) were administered at 25 mg/kg/day. Vehicle consisted of 5% DMSO, 40% PEG300, 5% Tween-80, and 45% saline. Anti-PD1 (BE0146), CTLA4 (BE0164), CD40 (BE0016), or rat IgG2a control antibodies (BioXCell) were administered on days 1, 3, and 5 of treatment at a dose of 20–30 μg each. All antibodies were diluted to the appropriate concentrations in 100 μL of sterile PBS (pH 7.4). Biochemical tests were performed within 2 days following the withdrawal period.

METHOD DETAILS

Normal and malignant human tissue samples were provided by the Stony Brook University BioBank. Paraffin-embedded 3 μm sections were processed and stained with hematoxylin and eosin. The following antibodies were used for IHC: rabbit polyclonal P-ERK, P-S6, CDH1, MKI67, CD3, and CD8 (Abcam), supported with services of iHisto (Salem, MA) and Stony Brook University Research Histology Core facility. Positive cells were counted at magnification of x200, and at least 10 fields per section for each sample were examined. For flow cytometry, the tumor tissue was dissociated using collagenase and hyaluronidase (Stem Cell Technologies) and DNase I (Sigma). The tissue was chopped into 1 mm pieces and incubated in an enzyme solution in DMEM at 37°C for 1 h. Live cells were scored using propidium iodide exclusion and stained with APC-conjugated antibodies to CDH1, EpCAM and Thy1 (eBioscience), and analyzed using FACSCalibur (BD). For single cell RNA sequencing, three pancreatic tumors derived from orthotopic transplantation into syngeneic mice were enzymatically dissociated into single-cell suspensions, followed by microfluidic partitioning into nanoliter droplets containing barcoded mRNA capture beads (Single Cell 3′ Reagent Kit v2; 10× Genomics). Single-cell barcoded cDNA libraries were prepared according to the manufacturer's protocol and sequenced on Illumina HiSeq 4000s (Novogene). Sequencing data were processed and analyzed by the 10× Genomics Cell Ranger pipeline (version 3.0.1) and Loupe Cell Browser v3.0.1.

QUANTIFICATION AND STATISTICAL ANALYSIS

Statistical analysis was performed using two-tailed Student's t test, ANOVA analysis, Fisher's exact test or Wilcoxon test, as appropriate for the dataset. An FDR adjusted *p*-value (q-value) was calculated for multiple comparison correction. Individual mice and tumor cell lines were considered biological replicates. Statistical details for each experiment are denoted in the corresponding figures and figure legends. Micrographs (H&E and IHC images) represent at least three independent experiments. For the quantification of IHC, the number of fields is indicated and *p* values between two groups were determined using the two-tailed t-test at the 0.05 confidence interval. The data are presented as the mean ± SD.